ICONHIC 2016
1st International Conference on Natural Hazards & Infrastructure
28-30 June, 2016, Chania, Greece

Canyon Depth Effect on Surface Ground Motion

E. Skiada[1], S. Kontoe, P.J. Stafford, D.M. Potts
Imperial College London

ABSTRACT

Topographic effects are rarely accounted for in seismic design codes, despite their potential to significantly modify surface ground motions. This paper investigates the influence of a canyon's slope height on the surface ground motion through a parametric time-domain Finite Element (FE) study. A two-dimensional plane-strain model of an idealised canyon is considered for vertically propagating SV waves, using wavelets as input excitation. The model consists of two step-like slopes with slope height (H), in a homogeneous linear elastic soil layer overlying rigid bedrock. The analysis results show that the distribution of topographic aggravation at the ground surface varies significantly with normalized canyon depth over the input wavelength (H/λ) and it does not necessarily reach a maximum at a specific H/λ ratio, as has been suggested in previous studies. The validity of this conclusion is investigated for different depths to bedrock and soil layer properties.

Keywords: topography, 2D wave propagation, amplification, slopes

INTRODUCTION

The substantial effect of surface topography on earthquake ground motion is well-known especially that associated with convex areas at the ground surface during destructive earthquakes. Observations from past events, e.g., Northridge 1994, Athens 1999, Haiti 2010 and Christchurch 2011, and numerical studies have shown that seismic ground motion is mainly amplified around hills, ridges and at the crests of slopes. The majority of previous numerical studies consider topographic irregularity as an isolated feature in a homogeneous elastic half space and usually obtain amplification factors smaller than those from field observations - typically 2-3 times the free-field motion (Pedersen *et al.*, 1994) - compared with amplification magnitudes ranging from 2 to 10 and reaching values up to 30 times reported in the literature (Geli *et al.*, 1988). This difference was attributed to the numerical models' simplicity as they consider idealized isolated topographic features with homogeneous soil properties. However, in reality the actual geometry of the geological structures was more complicated. The investigated ridges were not isolated but there was a series of subparallel topographic features on site. Numerical model complexity, presence of subsurface soil layering, topographic and soil amplification interaction have been identified also by other researchers (Assimaki and Jeong, 2013) as possible reasons for these discrepancies.

However, topographic effects are rarely accounted for in design codes. The French seismic code (PS 92, 1999) has a provision for the topographic effects of slopes and ridges, while Eurocode 8 considers these effects to be significant for geometric irregularities of slope heights larger than 30m. Furthermore, a number of studies have shown that topographic amplification is maximised for a normalized slope crest height (H) to input wavelength (λ) ratio of around H/λ =0.2 (Ashford *et al.*, 1997; Bouckovalas and Papadimitriou, 2005). In this paper the

[1] Corresponding Author: E. Skiada, *Imperial College London, evangelia.skiada11@imperial.ac.uk*

validity of this latter observation is investigated in conjunction with the seemingly arbitrary slope height of 30m which is suggested in EC8.

METHODOLOGY

Two-dimensional time-domain finite element analyses were performed, considering a canyon in a soil layer over rigid bedrock subjected to vertically propagating in-plane shear (SV) waves. The soil is treated as a homogeneous linearly elastic material, with properties listed in Table 1. The Finite Element (FE) model geometry consists of a canyon of height (H), slope inclination angle (i) and soil layer thickness (z), as presented in Fig.1. The first set of parametric analyses focuses on the impact of the normalised wavelength (H/λ) on the response by varying both the input motion wavelength (λ) and the slope height (H). The mesh width (L=500m) and the slope inclination angle (i=90°) were fixed for the current study. A second set of parametric analyses was performed, varying the soil layer's fundamental frequency using different values for the bedrock depth (z) and the crest-to-crest distance (L_{ctc}) of the two slopes forming the canyon sides. The variation of the latter two parameters was examined to confirm that the conclusions of the first parametric study are also valid for other problem geometries. Results of this paper focus only on the depth to bedrock (z) variation. Crest-to-crest distance variation is discussed in Skiada *et al.* (2017).

All numerical analyses were carried out with the Imperial College Finite Element Program, ICFEP (Potts and Zdravković, 1999) employing the generalised-α time integration scheme of Chung and Hulbert (1993). This scheme is an unconditionally stable implicit method with second order accuracy and controllable numerical damping, Kontoe *et al.* (2008). In all analyses the time-step is defined as a fraction of the predominant period of the input motion ($\Delta t=T_p/40$). The largest element dimension, Δl, of the mesh follows the Kuhlemeyer and Lysmer (1973) recommendation of $\Delta l \leq \lambda_{min}/10$, where λ_{min} is the wavelength determined for the largest frequency of all the input pulses that were considered, to ensure accurate wave transmission across the mesh.

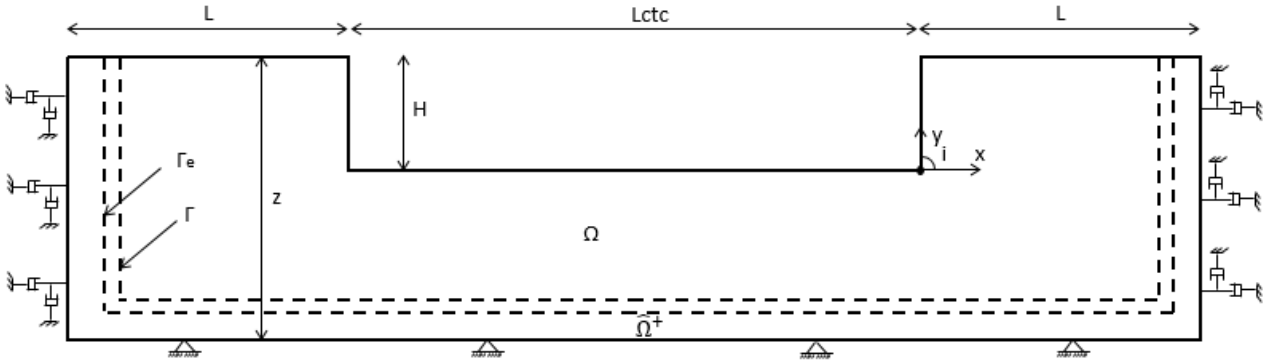

Figure 1. Considered FE canyon geometry.

Table 1. Considered soil parameters.

Modulus of elasticity, E	1333MPa
Mass density, ρ	2.0 Mg/m^3
Poisson's ratio, ν	1/3
Horizontal coefficient of earth pressure, K_o	1.0
Damping ratio, ξ	5% (achieved by varying Rayleigh damping parameters)

Concerning the location of the FE mesh boundaries, the distance of the bottom and lateral boundaries of the problem needs to be decided, so as the solution is not affected by the boundary conditions (BCs). The bottom boundary location is determined based on the bedrock location. The Domain Reduction Method (DRM) was used to reduce the computational domain and to insure free-field conditions were obtained at the lateral boundaries of the FE mesh. This method is a two-step procedure, developed by Bielak *et al.* (2003) for seismological applications which can be used to reduce the size of the domain to be analysed (Kontoe *et al.*, 2009). During the first step (Step I), a simplified model is considered, consisting of the source and path

characteristics rather than the detailed simulation of the local site conditions. The computational cost of the Step I analysis is very small compared with analysing the whole domain, since geological features and structures at the area of interest are neglected. The second step (Step II) focuses on the reduced domain (area) of interest and an external region ($\widehat{\Omega}^{+}$). Equivalent forces calculated from the displacement field computed during Step I, are implemented as an input along the line Γ in Step II (Fig.1). The perturbation of the external area is only outgoing and corresponds to the relative response between Steps I and II. Free-field conditions can be accurately represented in the numerical model of Step II by introducing the domain reduction method (DRM) together with the standard viscous boundary (SVB) of Lysmer and Kuhlemeyer (1969) at the lateral boundaries. In Step I of the analysis, a soil column of thickness z and width of 2m was used and a horizontal acceleration time history was applied at the base of the mesh, while the vertical movement along the lateral boundaries and the base was restricted. In Step II, the SVB was applied along the lateral boundaries and both horizontal and vertical displacements were restricted along the bottom boundary to represent the rigid bedrock assumption.

An artificial acceleration, a(t), given by Equation 1 was applied to the base of the finite element mesh. This is a Chang's wavelet and is the same as the excitation used by Bouckovalas and Papadimitriou (2005). A maximum amplitude of unity was achieved by varying the constants of Equation 1

$$a(t) = \sqrt{\beta e^{-at} t^{\gamma}} \sin\left(\frac{2\pi t}{T_p}\right) \tag{1}$$

where α, β, and γ are constants controlling the shape and amplitude of the acceleration-time history, T_p is the predominant period of the pulse and t is time. The same number of cycles of the input motion was maintained regardless of the examined input frequency. A plot of the acceleration-time history of the input motion is shown in Fig.2. Acceleration time-histories at discrete points on the ground surface were obtained as the main output of the analysis. The free-field motion corresponding to the crest stratigraphy was used for the Step I column analyses (*i.e.*, the 1D model thickness for Step I was considered as z).

Topographic effects are numerically assessed by de-coupling them from the soil layer effects. For this reason, results from the 2D seismic response analyses accounting for both topographic and soil layer amplification are compared with 1D column analyses results which represent the free-field response and account for soil layer amplification. The topographic amplification factor is usually determined as the ratio of 2D and 1D (column) peak ground acceleration values or as the ratio of 2D and 1D Fourier spectra motions at the ground surface. For this study, the ratio of the peak horizontal ground accelerations A_h is considered in order for the amplification factors to be comparable to Ashford *et al.* (1997), Bouckovalas and Papadimitriou (2005) and Tripe *et al.* (2013) who all used this definition.

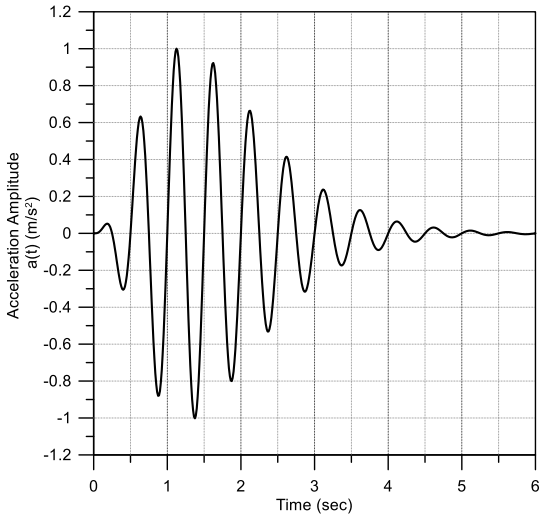

Figure 2. Chang's input motion for input period T_p=0.5sec (with considered α=4, β=50 and γ=5).

ANALYSIS RESULTS

Initially, the slope inclination (i), the depth to bedrock (z) and the crest-to-crest distance (L_{ctc}) are kept constant and only the slope height (H) and the input motion frequency are varied (changing T_p in Equation 1) in order to observe their effect on the topographic aggravation at the ground surface. The examined frequency range is 0.1Hz to 10Hz. As presented in Table 2, three values of slope height (H) were examined, for two depths to bedrock (z). Numerical analysis results are presented in terms of the maximum absolute acceleration and the normalised horizontal aggravation (A_h) at the crest and the toe of the slopes. Normalised response for the crest refers to the ratio of the maximum horizontal acceleration at the crest of the slope resulting from the 2D numerical analyses to the maximum horizontal acceleration of the 1D soil column with height equal to the crest height (z), denoted as 1D crest. Equally, normalised response for the toe refers to the ratio of the maximum horizontal acceleration at the toe of the slope resulting from the 2D numerical analyses to the maximum horizontal acceleration of the 1D soil column with height equal to the toe height (z-H), denoted as 1D toe. Variation of the depth to bedrock values is only performed to prove that conclusions from this parametric analyses are valid for a range of values of the canyon geometry.

Table 2. Numerical model varied parameters

Numerical Analyses No	Slope height H (m)	Depth to bedrock z (m)
1 to 3	25, 50, 75	125
4 to 6	25, 50, 75	250

Absolute acceleration response

The first set of analyses was performed by varying the canyon depth (H) of the numerical model presented in Fig. 1. The absolute peak horizontal acceleration was recorded at several points on the ground surface, both inside and outside of the canyon. Results of maximum acceleration computed at the crest (x, y)=(0,H) and the toe (x, y)=(0,0) of the slope are presented in Fig.3 and Fig.4 for the considered depths to bedrock z=125m and z=250m respectively. Dotted, full and dashed lines denote slope heights of 25m, 50m and 75m respectively.

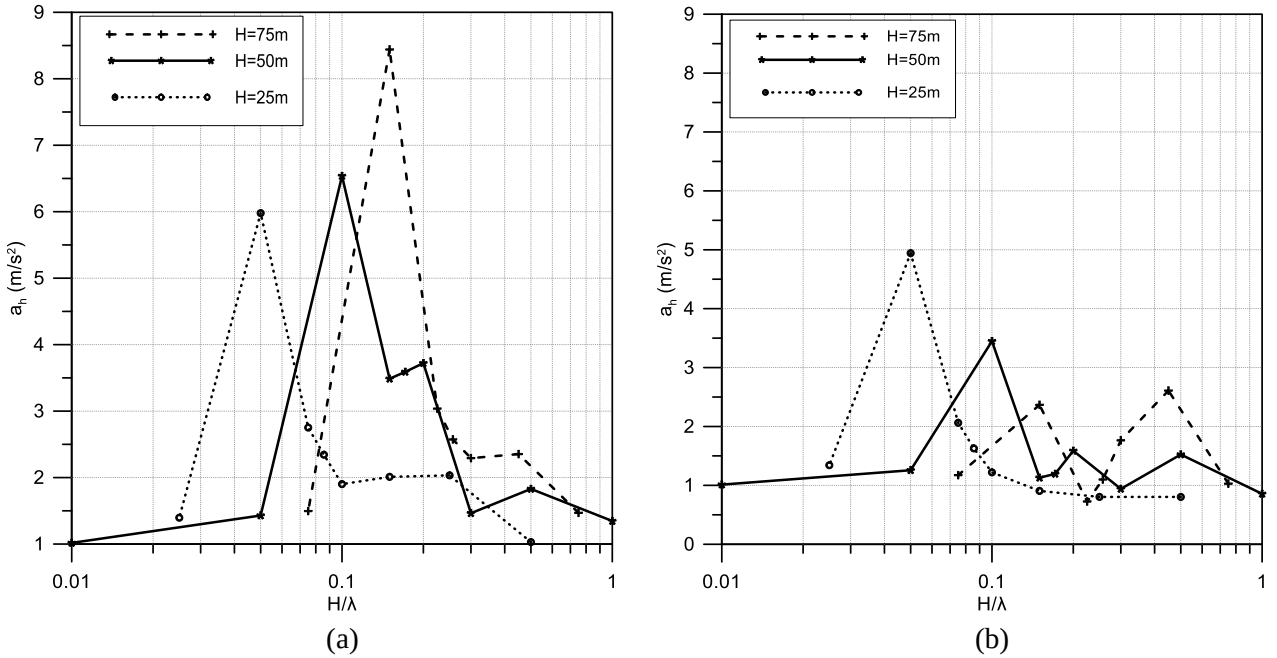

Figure 3. Crest (a) and toe (b) absolute maximum acceleration response for H=50m (full lines) in comparison with the H=25m (dotted lines) and H=75m (dashed lines) responses for z=125m.

Crest and toe maxima for the smaller examined depth to bedrock case (z=125m) in Fig.3 occur at H/λ=0.05, 0.1 and 0.15 for the H=25m, 50m and 75m respectively. All these ratios correspond to the same input motion period of T_p=1sec. Peak ground acceleration maximizes at that period, as the input motion period resonates with the first natural period of the crest and soil layer amplification dominates. The second peak of the toe response (Fig.3b) happens at H/λ=0.45 for a slope height of H=75m. This peak may still be due to the crest resonance with the input motion, because it happens at the second fundamental period of the crest (T_p=0.333sec). The same conclusions result from the larger depth to bedrock analyses of Fig.4. Maxima for slope heights of H=25m, H=50m and H=75m happen for H/λ ratios equal to 0.025, 0.05 and 0.075, which correspond to the first natural period of the crest (T_p=2sec).

As shown in Fig.3a for the shallow depth to bedrock case (z=125m), the acceleration at the crest increases with slope height. This trend is not observed for the deeper depth to bedrock case (z=250m, Fig.4a) where the peak response is similar for all the slope heights. Acceleration at the toe decreases with slope height for both the shallower and the deeper depth to bedrock cases (Fig.3b and Fig.4b respectively). This may be attributed to the topography of the slope because the shallower the canyon the more the problem resembles a site response problem for a soil layer of uniform height (z) above bedrock. Topographic amplification is occurring closer to the crest of the slope and de-amplification closer to the toe. Bearing this in mind, as the slope height increases, topography plays a more significant role in amplifying the crest response and de-amplifying the response at the toe.

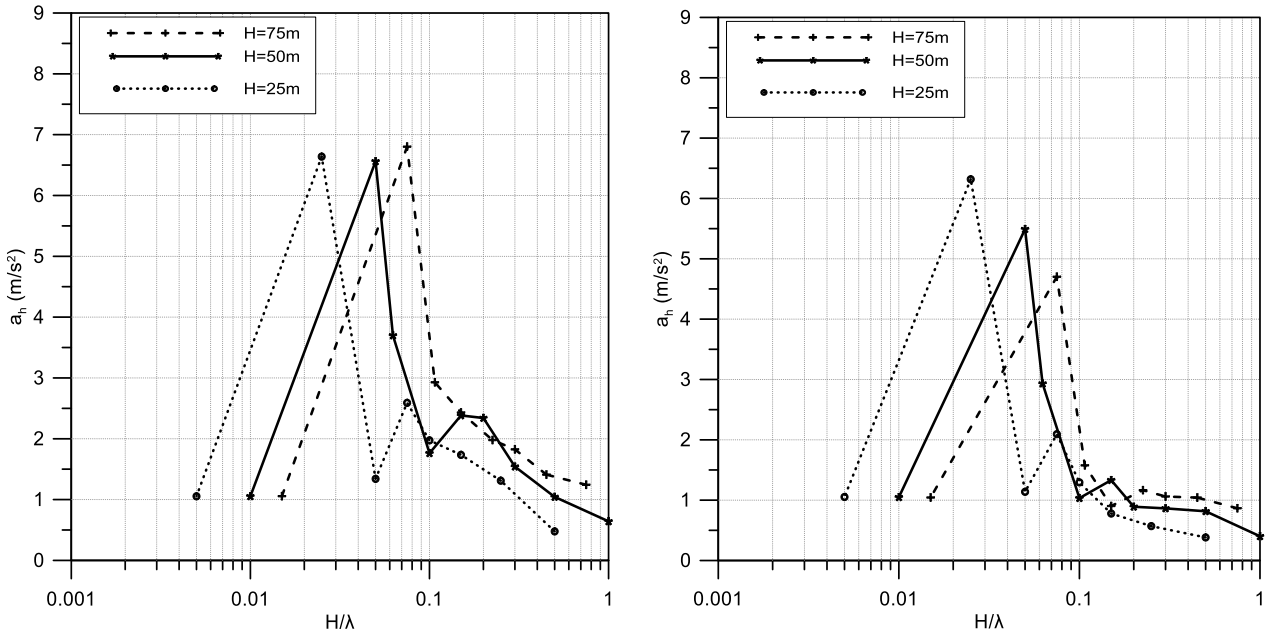

Figure 4. Crest (a) and toe (b) absolute maximum acceleration response for H=50m (full lines) in comparison to the H=25m (dotted lines) and H=75m (dashed lines) responses for z=250m.

Normalised acceleration response

The results presented in the previous section are repeated herein in normalised format. The maximum horizontal acceleration computed at the crest or the toe is normalised by the corresponding 1D maximum horizontal acceleration of the crest or the toe. This normalisation allows us to isolate the topographic effects on ground acceleration rather than the combined topographic and soil layer aggravation as seen previously in the absolute acceleration results. The crest response computed in this study (Fig.5a and Fig.6a) is superimposed on the results of Ashford *et al.* (1997) and Bouckovalas and Papadimitriou (2005) - full lines and separate points respectively - resulting from a step-like slope of height H=30m within an elastic half-space (*i.e.*, infinite depth to bedrock). Crest and toe maxima occur for different ratios of H/λ in this case, which was not the case in the previous section.

Crest maxima for slope heights of H=25m, 50m and 75m occur for ratios of H/λ=0.086, 0.2 and 0.3 for the small depth to bedrock case (z=125m) (Fig.5a). These H/λ ratios correspond to input motion periods of T_p=0.58sec, 0.5sec and 0.5sec. These periods are intermediate to the first and second natural periods of the 1D crest. In these intermediate periods the 1D crest soil layer amplification is low and therefore peaks appear in the 2D normalised response in that range. As the soil layer amplification is much smaller, it is easier for the topographic amplification to be observed. For the larger depth to bedrock case (Fig.6a, z=250m), the H=75m case gives a pronounced peak at T_p=1sec (H/λ=0.15) which is once more within the range of the first and the second natural periods of the 1D crest (T=2sec and 0.667sec respectively). Amplification peaks for the remaining two analyses, while happen in the same range, are not that significant. Similar to the smaller z case, these input motion periods are intermediate to the natural periods of the free-field crest response, leading to relatively low free-field acceleration, and hence to maximal normalized acceleration A_h values. The topographic amplification curve of the shallower slope case (H=25m of Fig.6a) is similar to the results given in Ashford *et al.* (1997) and Bouckovalas & Papadimitriou (2005). This is because the slope height is much smaller than the examined depth to bedrock value (z=250m) and the response is very similar to that of a single slope above a half space that has been examined by the above researchers.

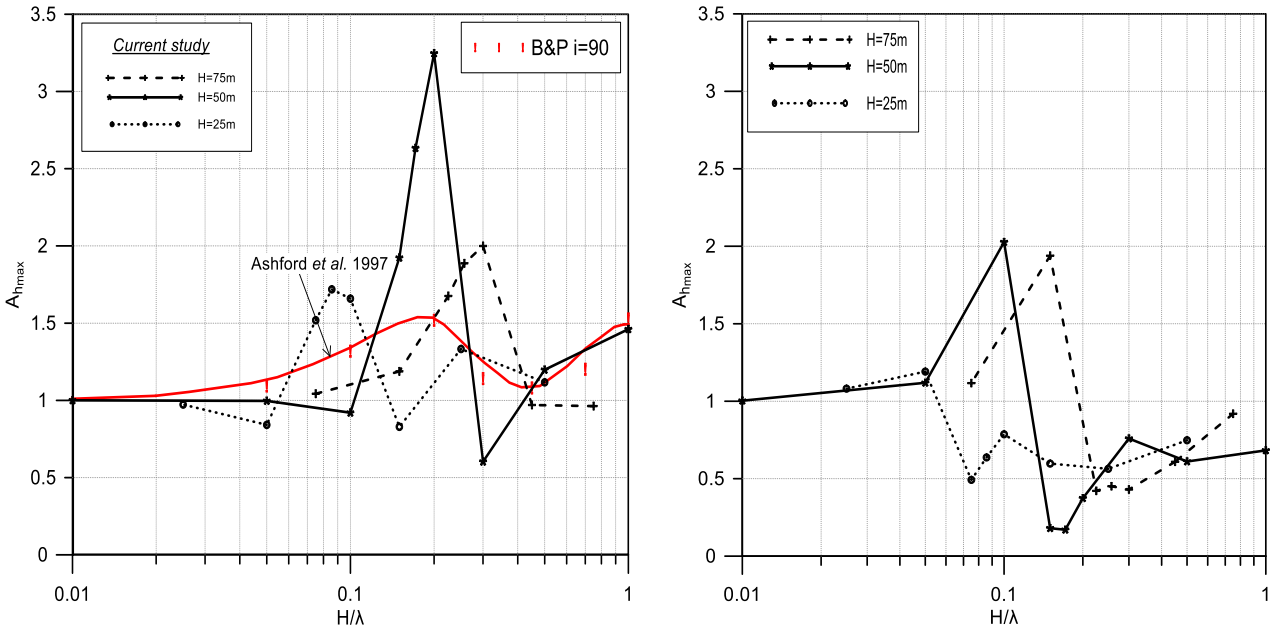

Figure 5. Crest (a) and toe (b) amplification response for H=50m (full lines) in comparison to the H=25m (dotted lines) and H=75m (dashed lines) responses for z=125m.

Toe normalized maxima occur at the same H/λ ratios as the absolute ones mentioned in the previous section for the intermediate and the largest examined slope heights (H=50m and 75m). This supports the conclusion that the crest resonance at specific input motion periods dominates the response by creating much larger soil amplification values compared to the topographic ones. The even smaller topographic aggravation of the toe compared to the crest area is difficult to capture in that case. Toe normalization is also misleading in this case because 1D soil columns of different heights (z-H) have been used to normalize the 2D results for the different examined slope heights, so aggravation values for the toe cannot be directly compared. Conclusions can only be made for the H/λ locations of the maximum topographic amplification. For H=25m, the slope is too shallow compared to the depth to bedrock of z=250m and the topographic effects are barely manifested (Fig.6b).

Since the locations of the normalised amplification peaks have not changed as compared to the non normalised ones (Fig.5b and Fig.6b in comparison to Fig.3b and Fig.4b respectively), a further investigation of the distribution of topographic amplification with distance from the slope was performed. Similar plots to those of Fig.5b were created for all the examined points at the canyon surface, focusing on the area inside the canyon (x<0, y=0). A similar response to that of the toe of the slope was observed for the points at the toe area with

the normalized amplification maxima occurring at the same H/λ ratios. The normalised acceleration is also plotted for several points across the canyon surface in Fig.7, focusing on the case with depth to bedrock z=125m and input motion period of T_p=1sec. This specific input motion period was chosen because it corresponds to the first natural period of the crest and as previously explained results in H/λ ratios where the toe normalized amplification peaks are observed. Horizontal distance is presented in a normalised format, with the origin of the horizontal axis located at the canyon centre.

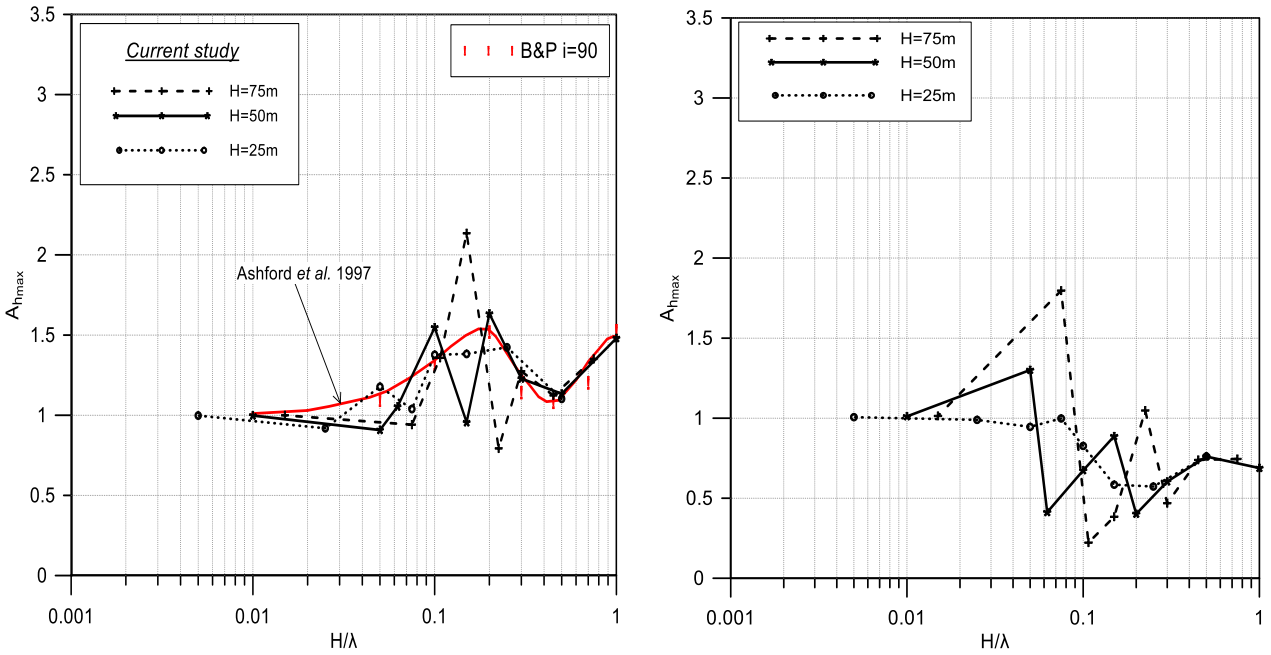

Figure 6. Crest (a) and toe (b) amplification response for H=50m (full lines) in comparison to the H=25m (dotted lines) and H=75m (dashed lines) responses for z=250m.

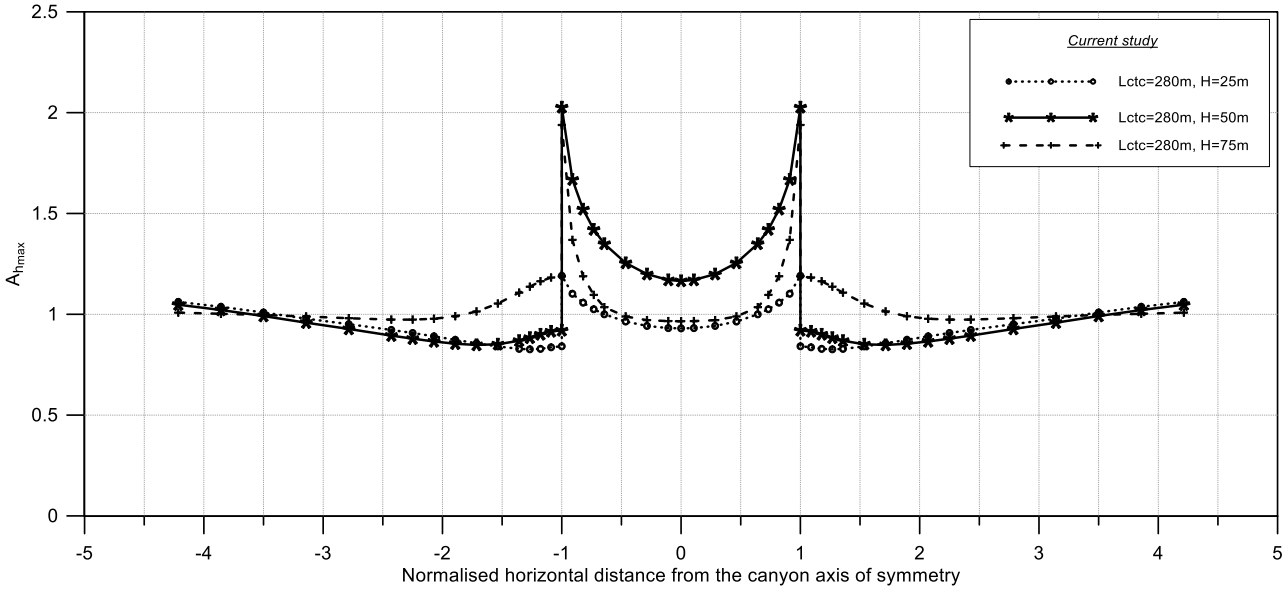

Figure 7. Maximum horizontal aggravation A_h with normalised distance from the canyon centre for several points on the ground surface for input motion period T_p=1sec.

Normalised response of points outside the canyon (behind the canyon crests) follows the crest normalisation while the response inside the canyon follows the same normalisation as that of the toe. As expected, larger amplification values are located closer to the topographic irregularity and become smaller with distance away

from the crest and the toe of the slope. However, response inside the canyon, and specifically at the toe area, is not only affected by the input motion period and the slope height, but strongly depends on the examined crest-to-crest distance. Due to this parameter affecting the results at the toe, further parametric analyses are considered necessary before a definite conclusion on the toe response can be made. Results of Fig.7 refer to a crest to crest distance of L_{ctc}=280m and further results for other canyon widths can be found in Skiada *et al.* (2017).

DISCUSSION

In this study, the maximum acceleration response for both the crest and toe locations is observed for different H/λ ratios, depending on the examined slope height H. However, in the literature, maximum topographic aggravation has been suggested to occur at H/λ values around 0.2 (Ashford *et al.*, 1997 and Bouckovalas and Papadimitriou, 2005). This can be attributed to the consideration of the same ratio of the slope height to the soil shear wave velocity (H/V_s) for the same range of the examined input motion frequencies considered in these studies. This maximum response at H/λ=0.2 has also been observed herein for H=50m, however the maxima shift depends on the examined slope height and can occur for much smaller H/λ ratios for smaller slope heights. The location in terms of H/λ values depends on the considered slope height (H), depth to bedrock (z) and considered shear wave velocity of the problem. Amplification maxima values are larger than those of Ashford *et al.* (1997) for all the examined cases. This is due to the considered layer over rigid bedrock condition in the current analyses in comparison to the half-space consideration of Ashford *et al.* (1997), as extensively discussed by Tripe *et al.* (2013).

Considering the cases examined in this study, amplification values are largest for H=50m and H=75m slope heights for depth to bedrock values of z=125m and z=250m respectively. This can be attributed to the relative dimension of the slope height (H) with respect to the depth to bedrock (z). For the case of H=25m, the slope height is comparatively small to the soil layer thickness above bedrock. The problem of shallow canyons is expected to have similar results to the homogeneous soil layer with uniform thickness (i.e. no canyon) overlying rigid bedrock. As a result, topography effects are expected to be less pronounced, which is also evident in the current study. As the slope height increases, topography and soil layer amplification interact and magnified aggravation is observed. The overall slope oscillation period is affected by the slope height (H), the depth to bedrock (z) and the considered shear wave velocity of the problem. In other words, topographic maxima happen at a specific H/λ value, not necessarily equal to 0.2, which depends on both the geometric and the soil characteristics of the problem.

CONCLUSIONS

This paper focuses on the effects of the canyon slope height on the surface ground motion amplification. For all the examined depth to bedrock cases, absolute peak ground acceleration values for both the crest and the toe points occur at the fundamental periods of the crest. Soil layer amplification dominates over topographic amplification in this case, due to resonance of the input motion period with the crest fundamental period. For larger examined values of the canyon slope height, larger acceleration values are observed at the crest area while smaller accelerations are observed at the toe. This is attributed to the larger scale of the topographic irregularity, which enhances the topographic effects on the ground surface.

Maximum normalised accelerations occur at periods that are intermediate to the natural periods of the crest. This is reasonable because topographic amplification can be easily observed in this period range, as the soil layer amplification is relatively low. In agreement with Ashford *et al.* (1997) and Bouckovalas and Papadimitriou, (2005), maximum topographic aggravation occurs at H/λ=0.2 for the examined slope height of H=50m. However, amplification peaks shift depending on the different examined slope heights. This study focuses on the prediction of the H/λ ratios where maximum amplification is expected, depending on the canyon geometry and specifically on the canyon slope height. Since code provisions have raised the significance of topography effects for larger slope heights, this parameter has been considered as very important on its effect on topographic aggravation of surface ground motion. A first approach to explain this parameter's significance was made by examining its relationship to changes of other geometrical characteristics of the numerical model,

like the depth to bedrock and the crest-to-crest distance parameters. However, further analyses need to be performed so that the role of these parameters can be sufficiently understood to enable the development of simplified expressions amenable to incorporation within design codes.

ACKNOWLEDGEMENTS

The first author would like to gratefully acknowledge the financial support by the Imperial College PhD Scholarships Program.

REFERENCES

Ashford SA, Sitar N, Lysmer J, Deng N. Topographic effects on the seismic response of steep slopes. *Bulletin of the Seismological Society of America* 1997, 87 (3): 701–9.

Assimaki D, Jeong S. Ground motion observations at Hotel Montana during the M7.0 2010 Haiti earthquake: Topography or Soils Amplification? Bulletin of the Seismological Society of America 2013, 103 (5): 2577-2590.

Bielak J, Loukakis K, Hisada Y, Yoshimura C. Domain reduction method for three-dimensional earthquake modelling in localized regions. Part I: theory. *Bulletin of the Seismological Society of America* 2003, 93 (2): 817–824.

Bouckovalas GD, Papadimitriou AG. Numerical evaluation of slope topography effects on seismic ground motion. *Soil Dynamics and Earthquake Engineering* 2005, 25: 547–58.

Chung J, Hulbert GM. A time integration algorithm for structural dynamics with improved numerical dissipation: the generalized-a method. *Journal of Applied Mechanics* 1993, 60: 371–5.

Eurocode 8: Design of Structures for Earthquake Resistance, Part 5: Foundations, retaining structures and geotechnical aspects, Annex A: Topographic Amplification Factors, EN1998-5:2004, 33.

Geli L, Bard P-Y, Jullien B. The effect of topography on earthquake ground motion: a review and new results. *Bulletin of the Seismological Society of America*, 1988, 78 (1): 42-63.

Kontoe S, Zdravković L, Potts DM. An assessment of time integration schemes for dynamic geotechnical problems. *Computers and Geotechnics* 2008, 35 (2): 253–64, http://dx.doi.org/10.1016/j.compgeo.2007.05.001.

Kontoe S, Zdravković L, Potts DM. The domain reduction method for dynamic coupled consolidation problems in geotechnical engineering. *International Journal for Numerical and Analytical Methods in Geomechanics* 2008, 32 (6): 659–80.

Kontoe S, Zdravković L, Potts DM. An assessment of the domain reduction method as an advanced boundary condition and some pitfalls in the use of conventional absorbing boundaries. *International Journal for Numerical and Analytical Methods in Geomechanics* 2009, 33: 309–30.

Kuhlemeyer RL, Lysmer J. Finite element method accuracy for wave propagation problems. Technical note. *Journal of Soil Mechanics and Foundation Division* 1973, 99 (5): 421–7.

Lysmer J, Kuhlemeyer RL. Finite dynamic model for infinite media. *Journal of the Engineering Mechanics Division, ASCE* 1969, 95 (4): 859–77.

Pedersen H, Le Brun B, Hatfield D, Campillo M, Bard P-Y. Ground motion amplitude across ridges. *Bulletin of the Seismological Society of America*, 1994, 84 (6): 1786-1800.

Potts DM, Zdravković L. Finite element analysis in geotechnical engineering. London 1999, Thomas Telford.

PS-92 Règles de construction parasismique: Règles PS applicables aux bâtiments, Normes NF P 06-013, Troisième Tirage, 1999.

Skiada E, Kontoe S, Stafford PJ, Potts DM. Canyon topography effects on ground motion. *16th World Conference on Earthquake Engineering (WCEE)*, Santiago, Chile, 2017.

Tripe R, Kontoe S, Wong TKC. Slope topography effects on ground motion in the presence of deep soil layers. *Soil Dynamics and Earthquake Engineering*, 2013, 50: 72-84.